Thermochimica Acta, 207 (1992) 161–175
Elsevier Science Publishers B.V., Amsterdam

Thermal analysis of controlled-release elastomeric formulations. Part 1. Determination of the solubility limits of sodium lauryl sulphate in elastomers by differential scanning calorimetry

E. Immelman and R.D. Sanderson

Institute for Polymer Science, University of Stellenbosch, Stellenbosch 7600 (South Africa)

(Received 20 December 1991)

Abstract

Controlled-release formulations for attaining long-term inhibition of bacterial oxidation of pyrite and the concomitant acid mine drainage were prepared from natural and synthetic rubbers used as binding matrices and sodium lauryl sulphate (SLS) as the active ingredient. The kinetics of release of an active agent from a polymeric matrix depend on several solute-dependent and solute-independent variables. This study focuses on one of the solute-dependent variables, namely, the solubility limit. Since no data on the solubility limits of SLS in natural and synthetic rubbers could be traced, techniques for determining these solubility values were investigated. In this study natural rubber (SMR 20) and synthetic *cis*-1,4-polyisoprene (IR-80) formulations containing from 0 to 35% SLS were analysed by differential scanning calorimetry (DSC). The thermograms obtained show the appearance of a characteristic melting endotherm when the solubility limit of SLS is exceeded, and this allows the amounts of dissolved and dispersed SLS in the controlled-release formulations to be estimated. The results of the study demonstrate the usefulness of DSC as a convenient and reliable method for determining the solubility limits of solids in elastomers.

INTRODUCTION

Acid mine drainage causes a pollution problem and is associated with the mining of coal and sulphide-containing minerals. The oxidation of fine-grained, reactive pyrite exposed during the mining process results in the production of acid and the solubilization of heavy metals [1–4]. Acid-contaminated waters are found wherever pyritic materials come into contact with air and water [5]. A bacterium *Thiobacillus ferrooxidans* accelerates the acidification of pyritic materials and increases the eventual level of

Correspondence to: E. Immelman, Institute for Polymer Science, University of Stellenbosch, Stellenbosch 7600, South Africa.

acid production by catalysing the oxidation of pyrite (FeS_2) to ferric sulphate [$Fe_2(SO_4)_3$] and sulphuric acid [1,2,5,6]. One approach to dealing with the problem of acid mine drainage is to reduce pyrite oxidation by inhibition of *T. ferrooxidans* [1,7–10]. Anionic surfactants, and in particular sodium lauryl sulphate (SLS) at low concentrations, are capable of inhibiting the activity of *T. ferrooxidans* [1,11,12]. In order to prevent repopulation by the bacteria, the bactericidal treatment must be repeated frequently or, alternatively, a continuous supply of the inhibitor must be available [1,4,12,13]. The latter can be accomplished by using controlled-release technology [14,15]. The inhibitor is incorporated into a polymeric matrix, from which it is released slowly into the aqueous environment by diffusion through the polymer matrix and dissolution from the surface of the controlled-release device. The continuous release of inhibitor from a controlled-release device should make the effective treatment of *T. ferrooxidans* possible for extended periods of time.

The development and laboratory evaluation of monolithic devices and membrane-controlled devices for the long-term inhibition of bacterial oxidation of pyrite have been reported in previous publications [16,17]. The kinetics of release of an active agent from a polymeric matrix depend on several solute-dependent and solute-independent variables [14]. The kinetics of release of SLS, and the influence of several solute-independent variables on the rate of release of SLS from monolithic elastomeric matrices, have been discussed [16]. The study reported here focuses on the experimental determination of one of the solute-dependent variables, namely, the solubility limit.

Monolithic devices are prepared by blending the active agent with the plastic or elastomeric material in the compounding step. The active agent dissolves in the plastic or elastomeric matrix until saturation is reached. Additional active agent remains dispersed within the polymeric matrix and the system is referred to as physically dispersed. The dispersed solute is in equilibrium with the dissolved solute, and the total concentration of active agent is designated as C_0 [14]. For monolithic devices containing dispersed solute, the following equation has been derived for the slab geometry [14,18]:

$$M_t \approx A(2DC_sC_0t)^{1/2} \qquad \text{for } C_0 \gg C_s \tag{1}$$

where M_t is the amount of agent released at time t, A is the surface area, D is the diffusion coefficient, C_0 is the total concentration of agent in the matrix, and C_s is the solubility of the agent in the matrix phase. The release rate at any time, dM_t/dt, is then given by

$$\frac{dM_t}{dt} \approx \frac{A}{2}\left(\frac{2DC_sC_0}{t}\right)^{1/2} \qquad \text{for } C_0 \gg C_s \tag{2}$$

From eqn. (2) it follows that the release rate of an agent from a monolithic device containing dispersed solute is proportional to the square root of the agent's solubility in the polymer, i.e. $C_s^{1/2}$.

Techniques which are frequently used for determining the solubility of solids in elastomers include scanning electron microscopy (SEM) [19] and X-ray fluorescence [20]. Solubility may also be determined by observation of certain physical properties of loaded panels. Usually, properties such as tensile strength and modulus show little change with agent loading until the solubility limit is reached. At that point there may be a dramatic variation, though not always [21]. Most of these techniques are time consuming and are often suitable for determining the presence or absence of solubility, rather than the actual solubility limit of a solid agent in an elastomer.

Since no data on the solubility limits of SLS in natural and synthetic rubbers could be traced, techniques for determining these solubility values were investigated. Attempts to determine the solubility limit of SLS in natural rubber by ^{13}C NMR analysis of rubber–SLS formulations were unsuccessful, since the spectra obtained for samples which contained 0%, 5%, 10% and 15% SLS were identical [22]. In the study reported here, natural rubber (SMR 20) and synthetic polyisoprene (IR-80) formulations containing from 0% to 35% SLS were analysed by DSC.

EXPERIMENTAL

Materials

Natural rubber (grade SMR 20) and synthetic *cis*-1,4-polyisoprene (grade IR-80) were supplied by Karbochem. Elastomer additives, namely, carbon black N220, zinc oxide, stearic acid, *N*-cyclohexyl-2-benzothiazole sulphenamide (ORAC CS), tetramethylthiuram disulphide (TMTD) and styrenated phenol antioxidant (OROX SP), were also supplied by Karbochem. Sodium lauryl sulphate (TEXAPON K12) and sublimed sulphur were purchased from Henkel South Africa (Pty) Ltd. and BDH Laboratory Reagents respectively.

Preparation of rubber masterbatch formulations

Two types of rubber masterbatch formulation were prepared, namely, natural rubber and synthetic polyisoprene, hereafter referred to as NR and IR respectively. The gum-stock rubber was softened by mechanical working on a two-roll rubber mill. Once it was in the softened state, vulcanization additives, carbon black and antioxidant were incorporated by further processing on the two-roll mill. The compositions of the two masterbatch formulations are given in Table 1.

TABLE 1

Compositions of rubber masterbatch formulations

Component	Formulation	
	A	B
Natural rubber (SMR 20) (parts)	100	
Synthetic *cis*-1,4-polyisoprene (IR-80) (parts)		100
Carbon black N220 (phr) [a]	9	9
Zinc oxide (phr)	5	5
Stearic acid (phr)	1	1
ORAC CS [b] (phr)	1.5	1.5
TMTD [c] (phr)	0.5	0.5
OROX SP [d] (phr)	2	2

[a] Parts per hundred parts of rubber.
[b] *N*-cyclohexyl-2-benzothiazole sulphenamide (accelerator).
[c] Tetramethylthiuram disulphide (accelerator).
[d] Styrenated phenol (antioxidant).

Preparation of rubber–SLS formulations

Controlled-release formulations were prepared by blending masterbatch formulations with SLS, using a Model PLE 651 Brabender Plasti-Corder (Brabender, Germany) and an adjustable-speed Brabender two-roll mill. Since an accelerated sulphur vulcanization system was used, sulphur (2 parts per hundred parts of rubber (phr)) was also added to masterbatch formulations at that stage of the mixing process. After addition of SLS and sulphur, blending was continued for about 20 min to ensure homogeneous dispersion of SLS in the rubber matrices.

Scanning electron microscopy

The microstructure of natural rubber–SLS samples which contained 0% and 35% SLS was studied before and after the release of SLS using SEM. Samples were frozen with liquid nitrogen, microtomed into thin sections, mounted on aluminium stubs, and sputter-coated with a thin layer of gold. SEM micrographs of the surfaces and cross-sections of rubber–SLS samples were taken using a Hitachi S-405A scanning electron microscope.

Determination of the solubility limits of SLS in elastomers

The solubility limits of SLS in NR and in IR were investigated by differential scanning calorimetry (DSC) using a Du Pont 9900 computer/thermal analyser and its Model 910 differential scanning calorimetry module. Indium metal was used as the calibration standard. DSC scans were done on SLS in order to determine its melting tempera-

ture. This was followed by DSC scans on NR and IR formulations which contained different loadings of SLS. Formulations containing from 0% to 35% (referring to mass percentage) SLS were analysed. In all analyses, the sample mass was 17.1 mg and the heating rate was 10°C min^{-1}. The objective of this investigation was to determine the level of SLS at which phase separation started, i.e. the level at which the solubility limit of the SLS in the rubber was exceeded. In addition to DSC analyses, the degradation temperature of SLS was determined by thermogravimetric analysis (TGA). This was done using a Du Pont Model 951 thermogravimetric analyser.

RESULTS AND DISCUSSION

A DSC scan of "pure" SLS showed a sharp endotherm at about 115°C, as shown in Fig. 1. Values for the melting point of SLS were difficult to trace, and values given in chemical catalogues were relied upon. According to the Aldrich Chemical Catalog [23], the melting point of SLS is 204–207°C. Thermogravimetric analysis of SLS showed that a mass loss of about 56% occurred at 227°C. This temperature was not much higher than the melting point given for SLS and indicated that SLS started to decompose soon after it melted. Heating of SLS in an open oven to 230°C did not lead to melting, but only to a charring of the surface. A TGA scan of SLS is shown in Fig. 2. A possible explanation for the appearance of a sharp endotherm at about 115°C (Fig. 1), instead of at about 204°C, is that the apparent crystalline phase transition at 115°C could have been related to the dual nature of the SLS molecule, i.e. the presence of both organic and inorganic groups in the same molecule. As Fig. 1 shows, a small endotherm also

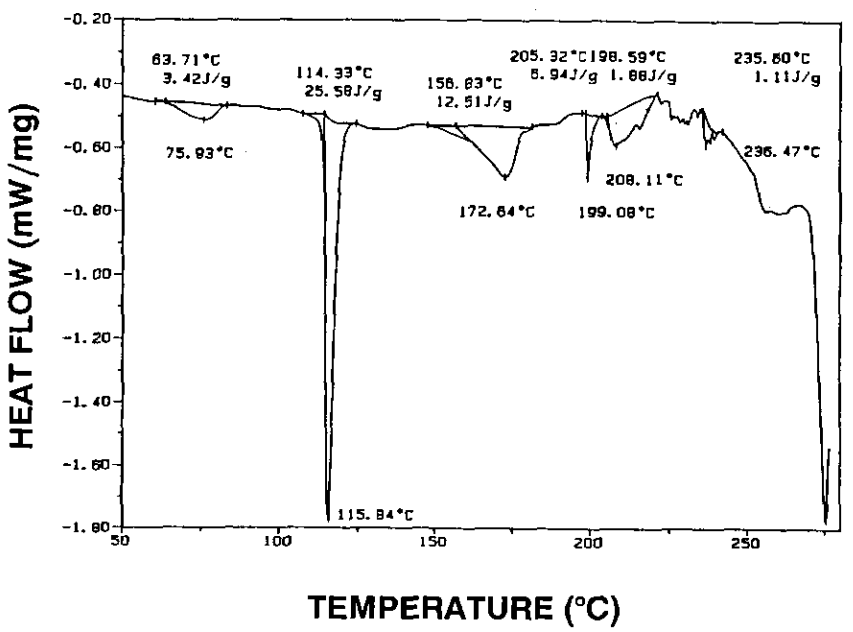

Fig. 1. DSC scan of sodium lauryl sulphate (Texapon K12), showing the endotherm at about 115°C.

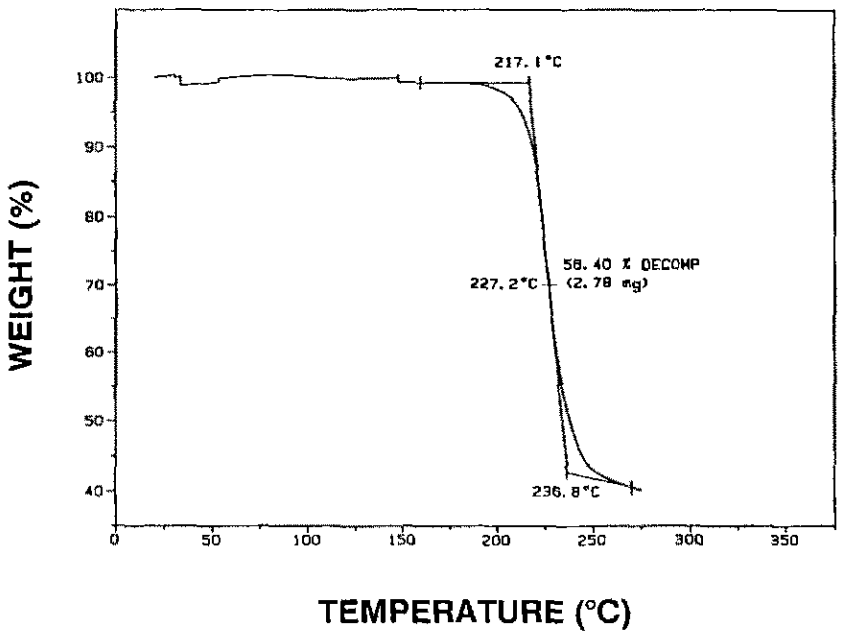

Fig. 2. TGA scan of sodium lauryl sulphate (Texapon K12).

appeared at about 205°C, with a peak temperature at 208°C. However, the heat of fusion for this endotherm was only 6.94 J g^{-1}, compared with 25.58 J g^{-1} for the endotherm at 115°C.

Subsequent DSC scans of NR samples with SLS contents which ranged from 0% to 35% showed the appearance of an endotherm at approximately 115°C for NR which contained 5% SLS. A sample of NR with an SLS content of 4% showed no sign of an endotherm at this temperature. These results indicated that at a level of 4% all the SLS was present as dissolved surfactant, whereas when the SLS was at a level of 5%, the solubility limit in NR was exceeded and some SLS was present as dispersed particles. Phase separation therefore occurred at an SLS level of 5%, i.e. SLS was not compatible with the rubber at this level. The endotherm observed at about 115°C for NR which contained 5% SLS was the result of a phase

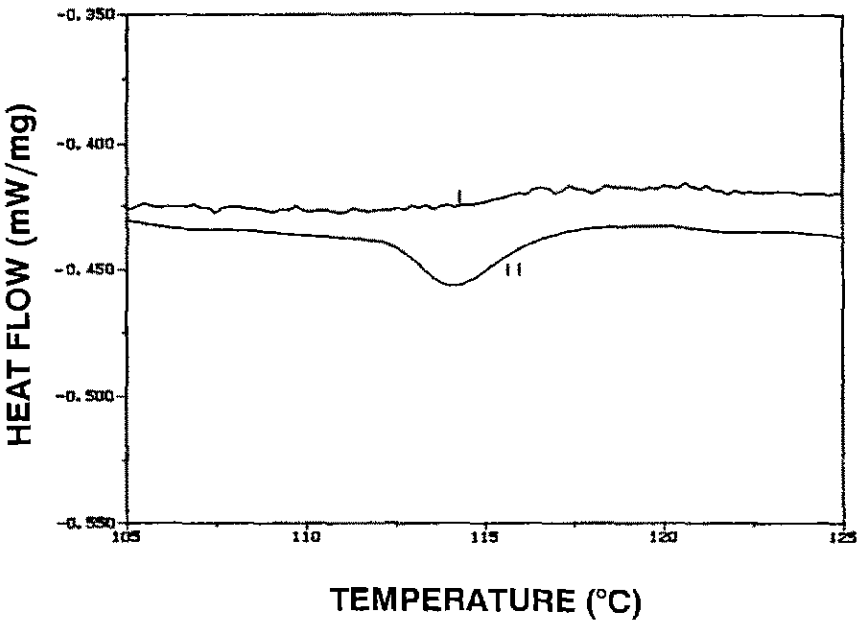

Fig. 3. DSC scans of natural rubber containing 4% SLS (curve I) and 5% SLS (curve II).

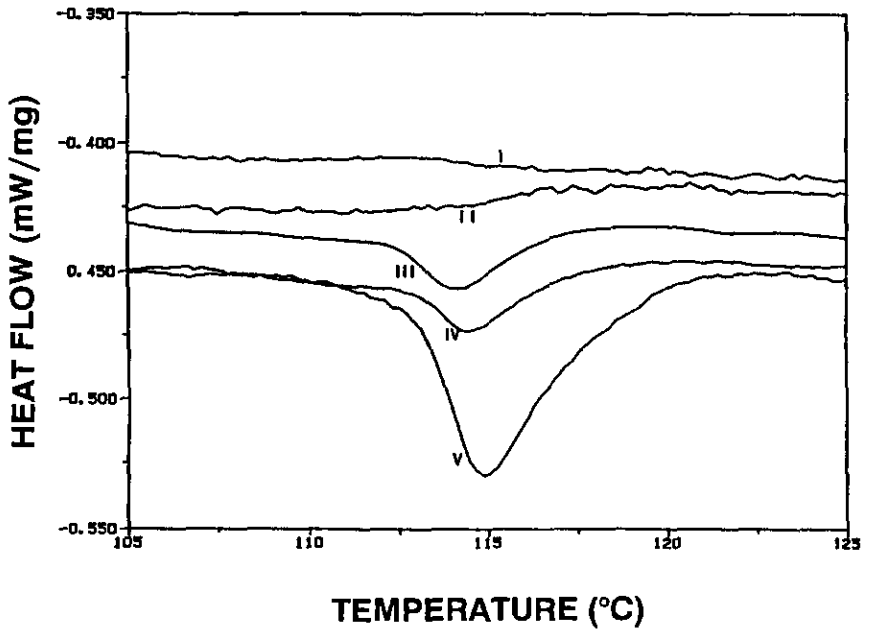

Fig. 4. DSC scans of natural rubber containing 0% SLS (curve I), 4% SLS (curve II), 5% SLS (curve III), 6% SLS (curve IV) and 10% SLS (curve V).

transition in the dispersed solid SLS particles. DSC thermograms of NR which contained 4% and 5% SLS are shown in Fig. 3. The appearance of an endotherm at about 115°C was more pronounced in NR which contained, for example, 6% and 10% SLS, as shown in Fig. 4.

An increase in the SLS content resulted in an increase in the area of the endotherm, as illustrated in Fig. 5. Samples which contained 25% and 35% SLS (Fig. 5) showed that most of the SLS was present as a separate phase, i.e. as dispersed solid particles. The broad endotherms observed for these samples, as opposed to the sharp endotherm for SLS (Fig. 1), could be attributed to interference with the phase transition due to dispersion of the SLS in the rubber matrix. Scanning electron micrographs of the surfaces of samples which contained 0% and 35% SLS are shown in Figs. 6 and 7

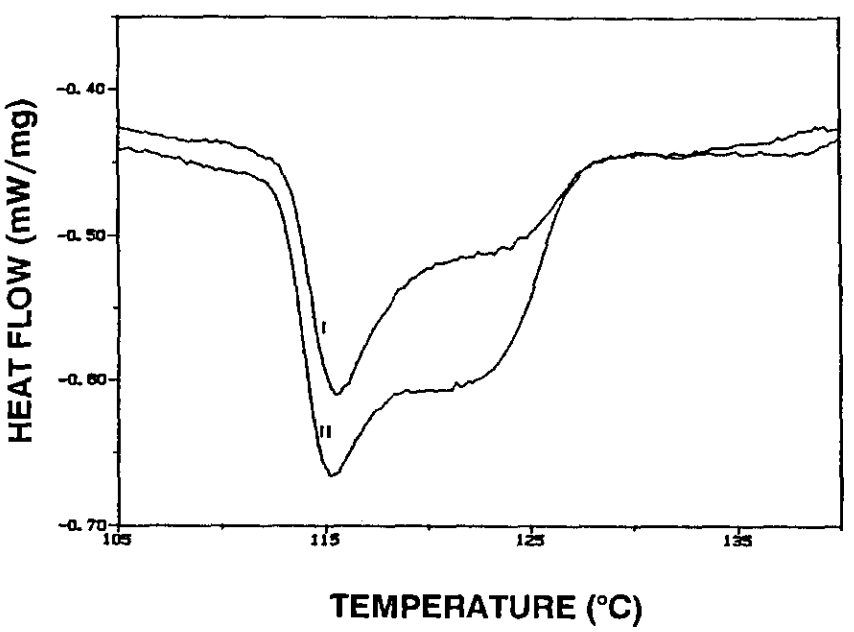

Fig. 5. DSC scans of natural rubber containing 25% SLS (curve I) and 35% SLS (curve II).

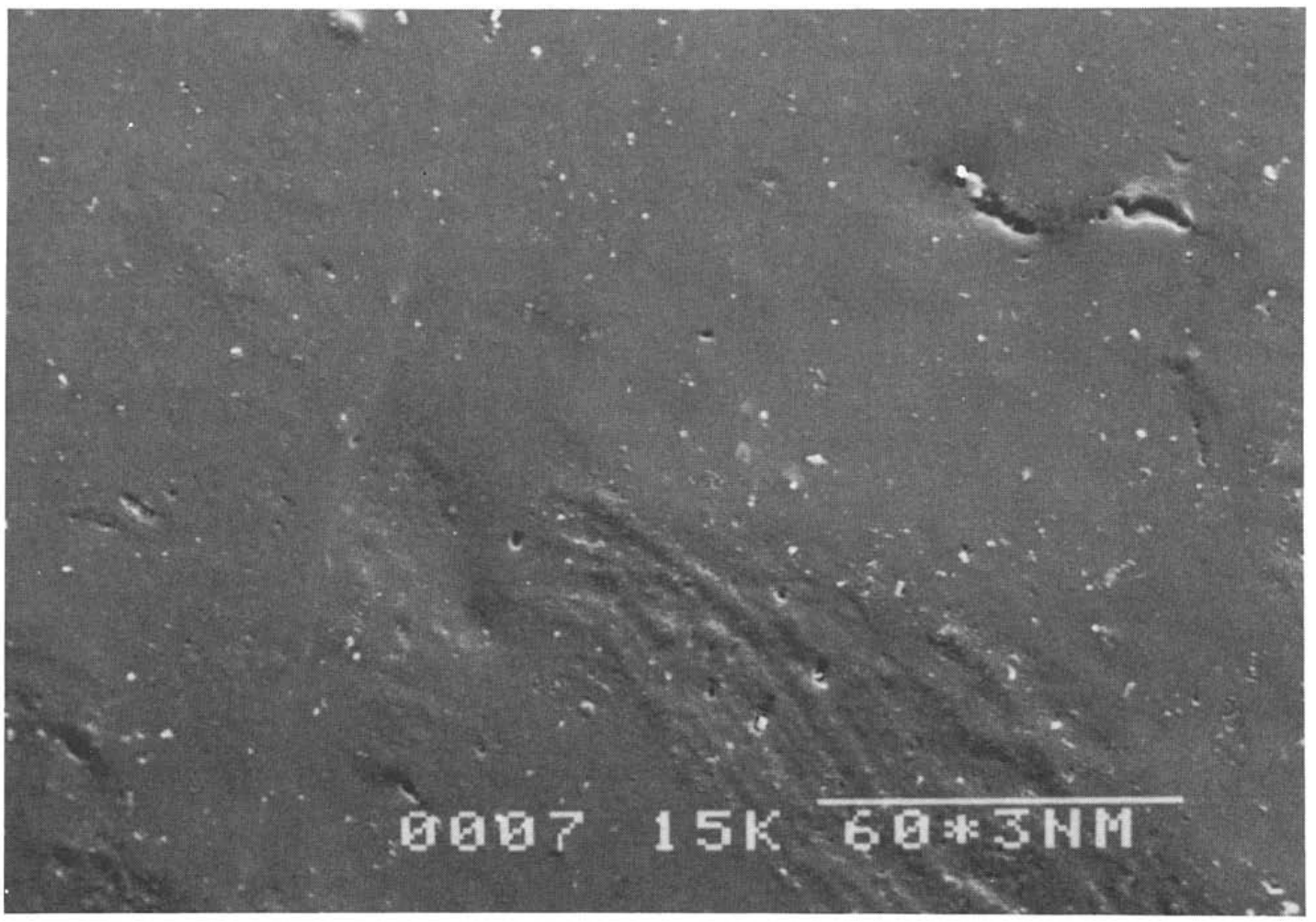

Fig. 6. Scanning electron micrograph of the surface of an NR sample which contained no SLS.

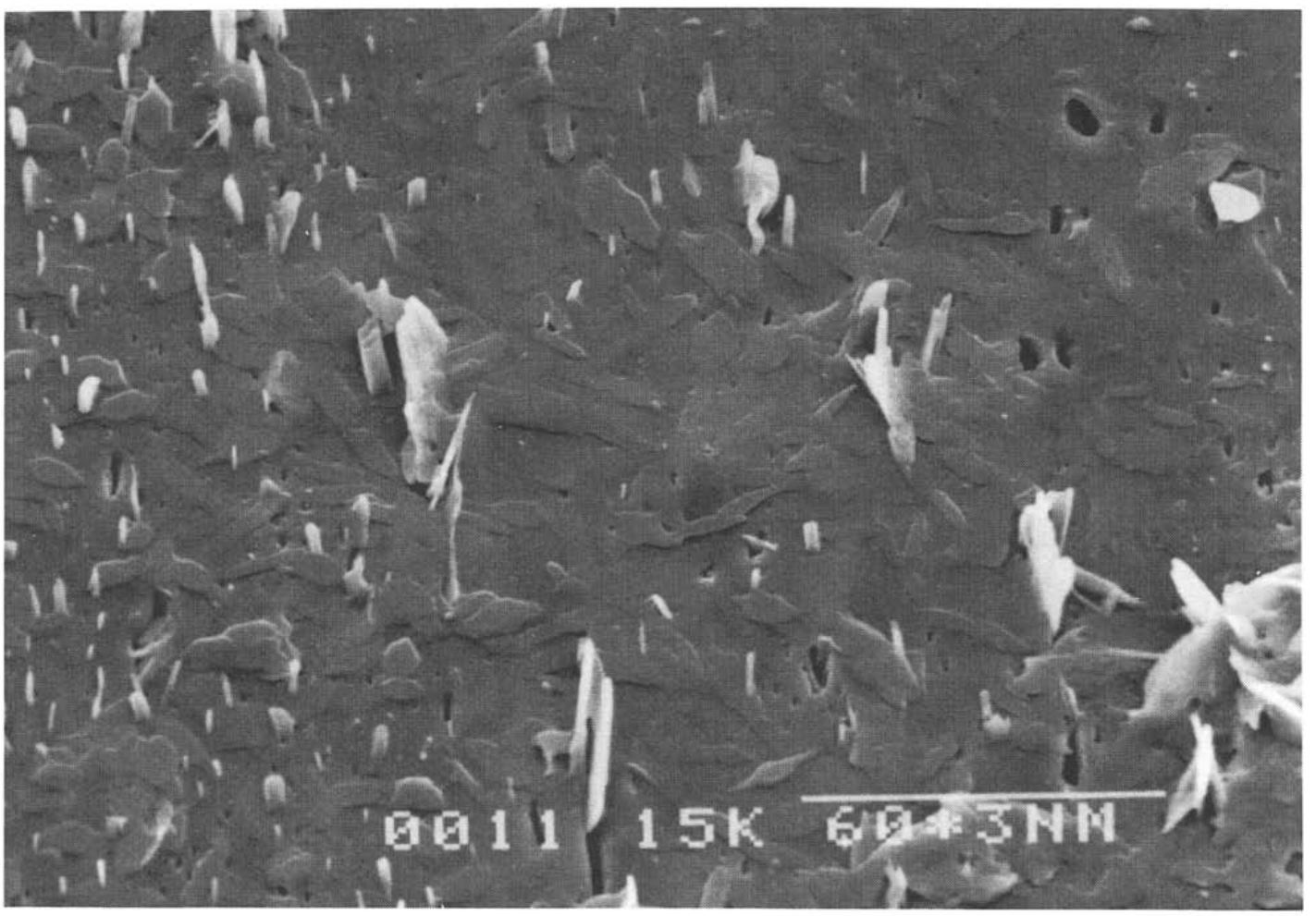

Fig. 7. Scanning electron micrograph of the surface of an NR/35% SLS sample, showing the change in the surface texture due to incorporation of dispersed SLS particles.

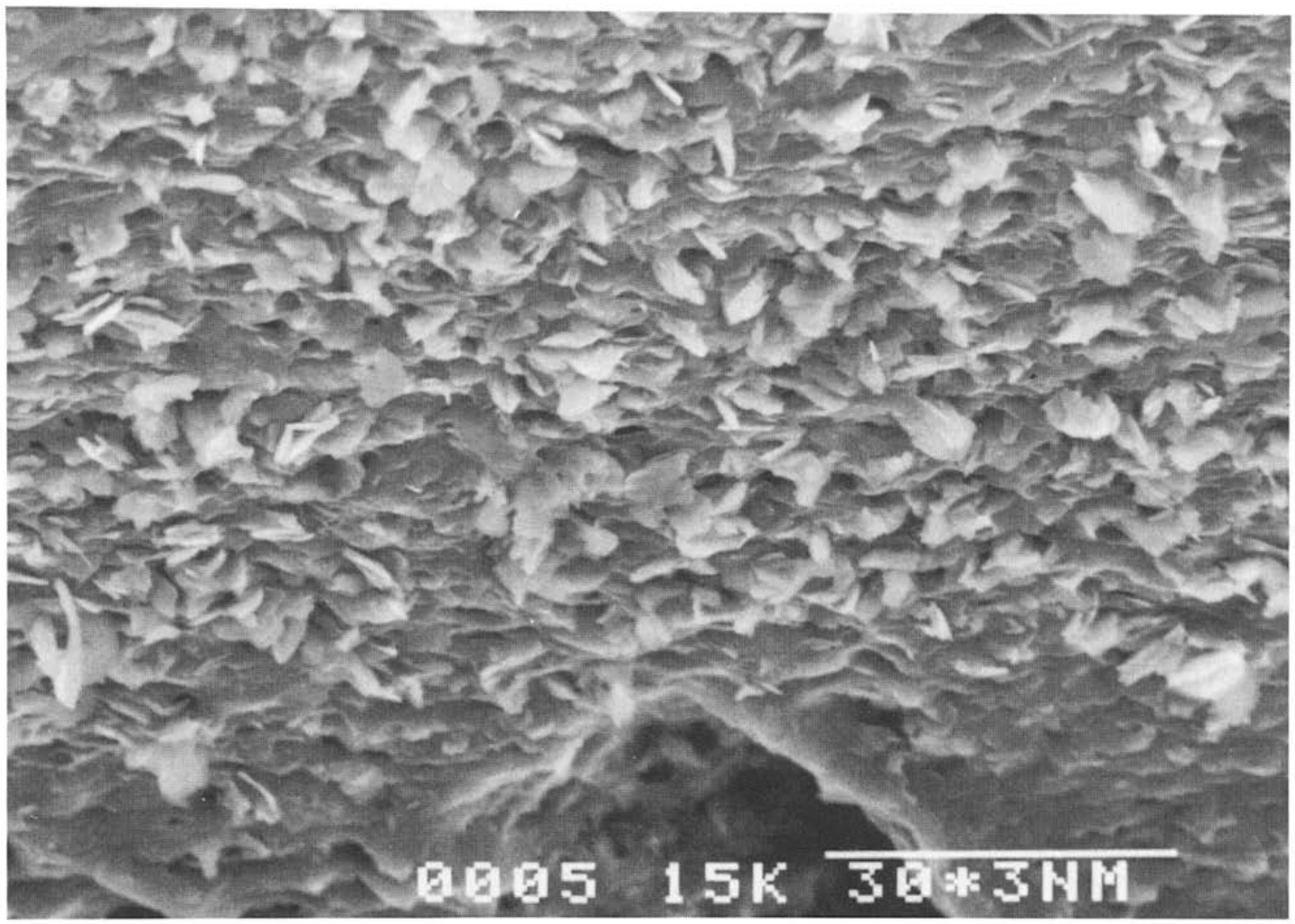

Fig. 8. Scanning electron micrograph of a cross-section of an NR/35% SLS sample, showing the dispersed SLS particles in the rubber matrix.

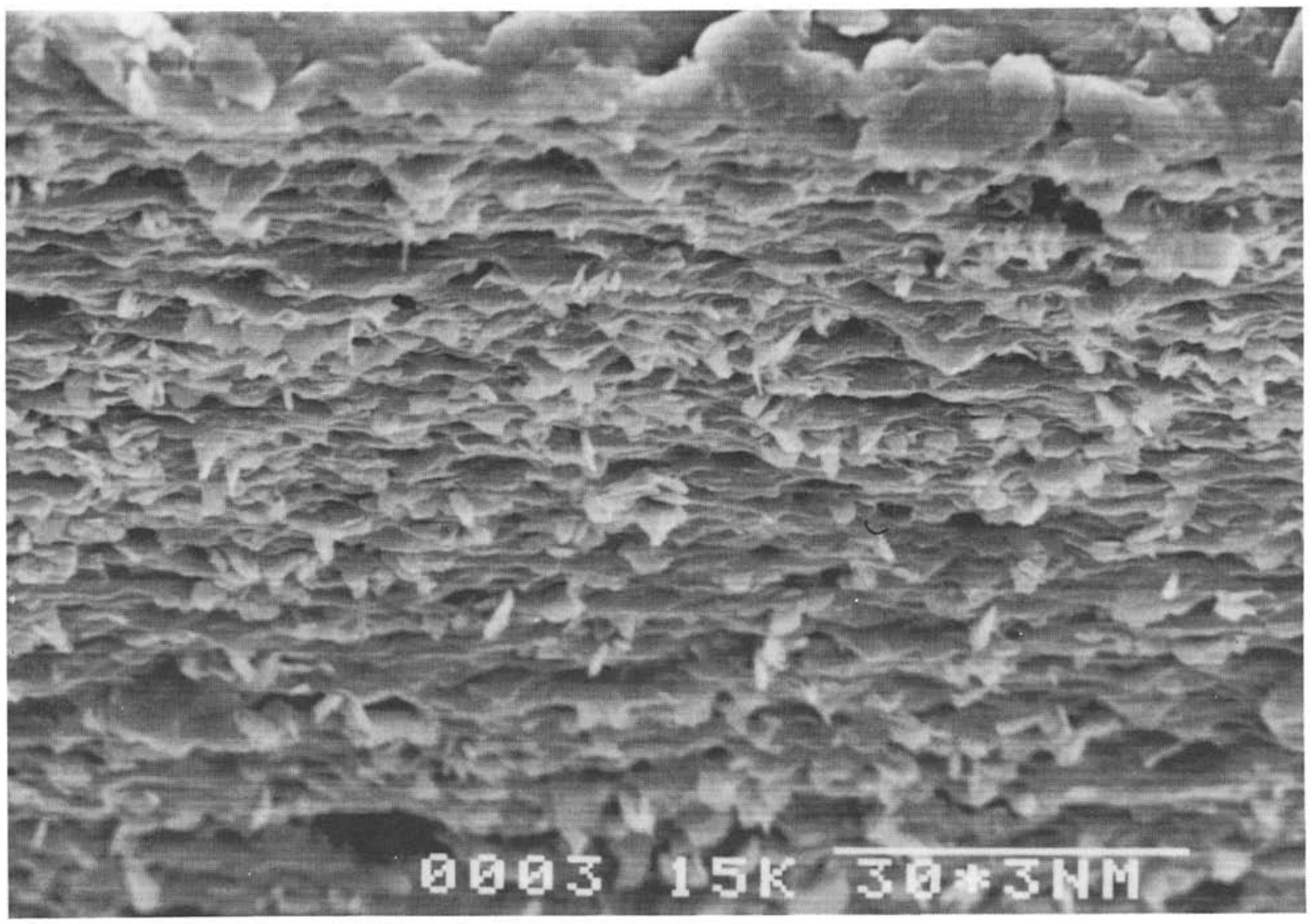

Fig. 9. Scanning electron micrograph of a cross-section of an NR/35% SLS sample, showing the dispersed SLS particles in the rubber matrix, as well as at the sample surface (top).

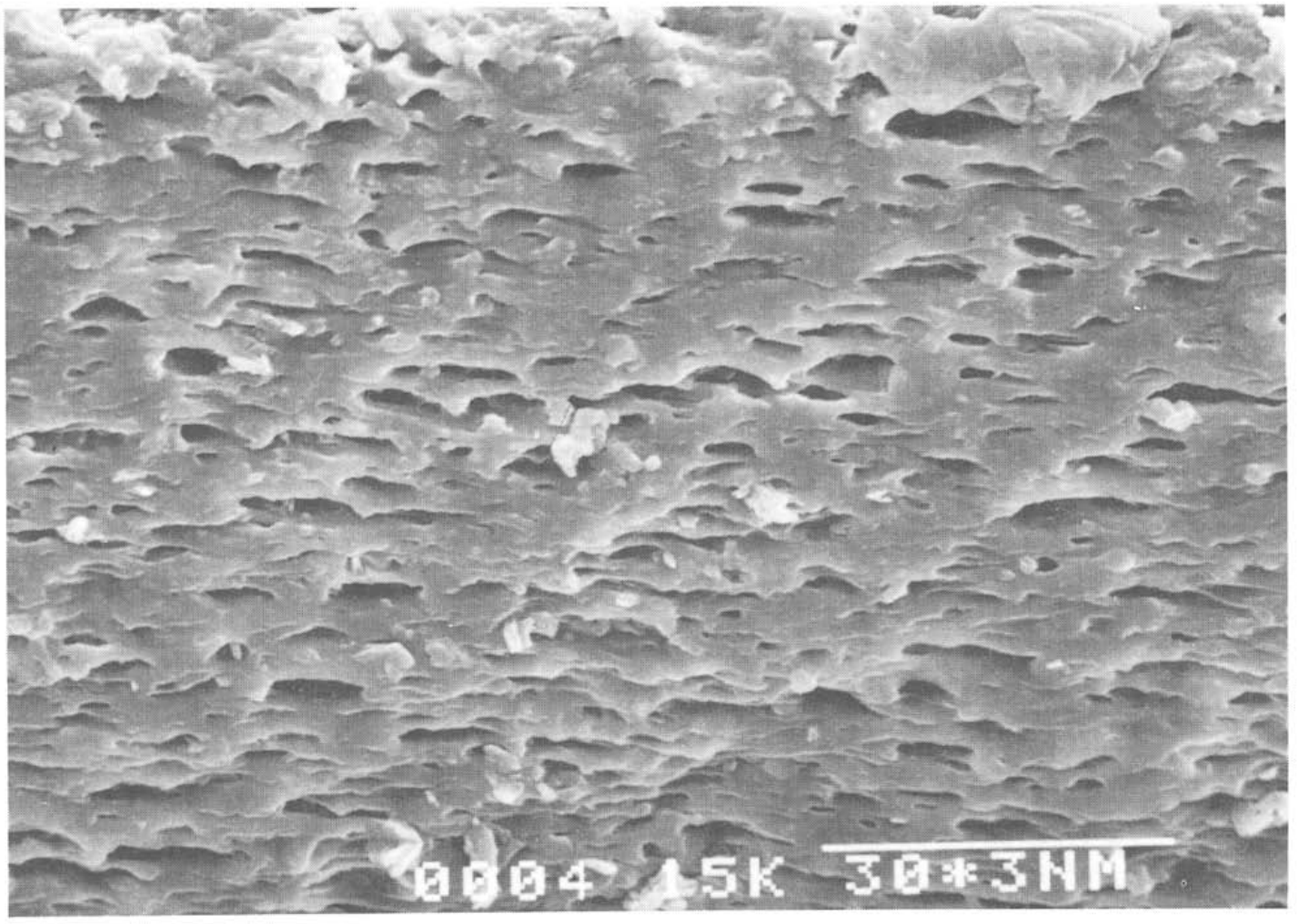

Fig. 10. Scanning electron micrograph of a cross-section of a leached NR/35% SLS sample, showing the porosity created in the rubber matrix after release of large amounts of SLS.

respectively. Figures 8 and 9 show cross-sections of NR samples which contained 35% SLS. The large amount of dispersed SLS particles is clearly visible in these micrographs. A cross-section of a leached NR-35% SLS sample is shown in Fig. 10. The porosity created in the rubber matrix after

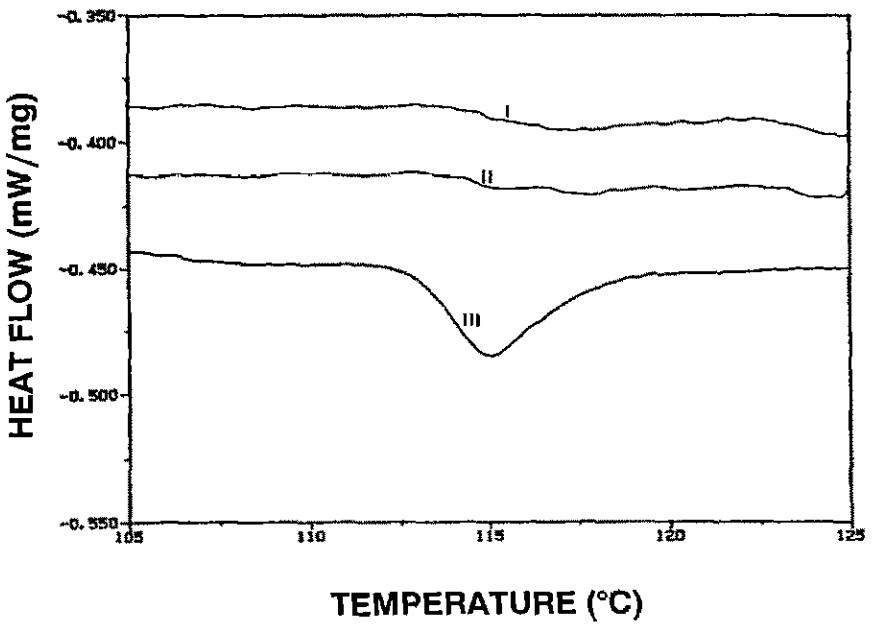

Fig. 11. DSC scans of synthetic polyisoprene containing 0% SLS (curve I), 3% SLS (curve II) and 4% SLS (curve III).

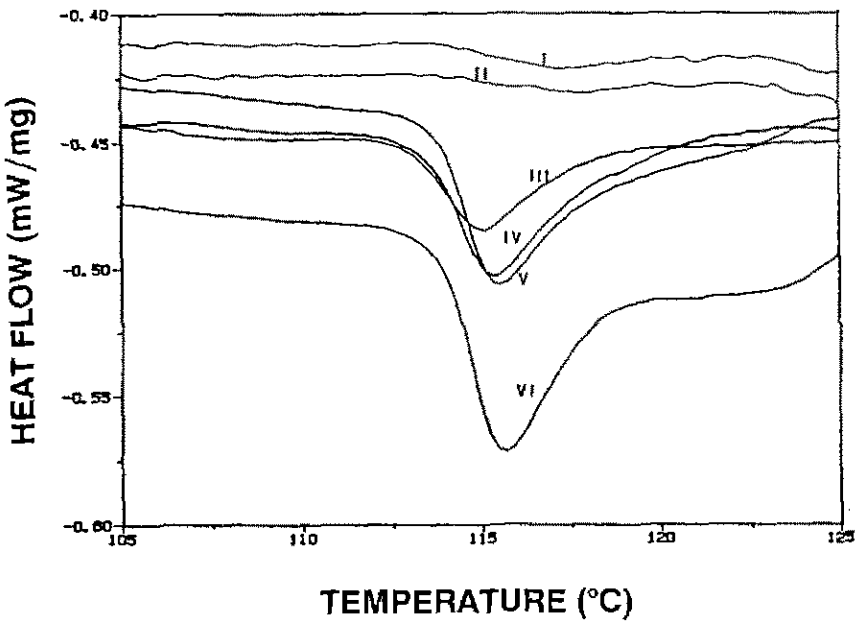

Fig. 12. DSC scans of synthetic polyisoprene containing 0% SLS (curve I), 3% SLS (curve II), 4% SLS (curve III), 6% SLS (curve IV), 8% SLS (curve V) and 10% SLS (curve VI).

the release of dispersed SLS particles is clearly shown in this micrograph.

DSC thermograms of IR with SLS contents which ranged from 0% to 35% showed that phase separation started at a level of 4% SLS, which suggested that the solubility limit of SLS in IR was 3%. This is illustrated in Fig. 11. As with NR, an increase in the SLS content of IR samples resulted in an increase in the area of the endotherm. This is shown in Fig. 12 for IR formulations which contained 4%, 6%, 8% and 10% SLS. All the NR and IR samples referred to in the above discussion were stored at 0°C after being compounded. Before they were analysed, these samples were removed from the freezer and allowed to equilibrate at room temperature for approximately 24 h. DSC analysis of NR samples which contained

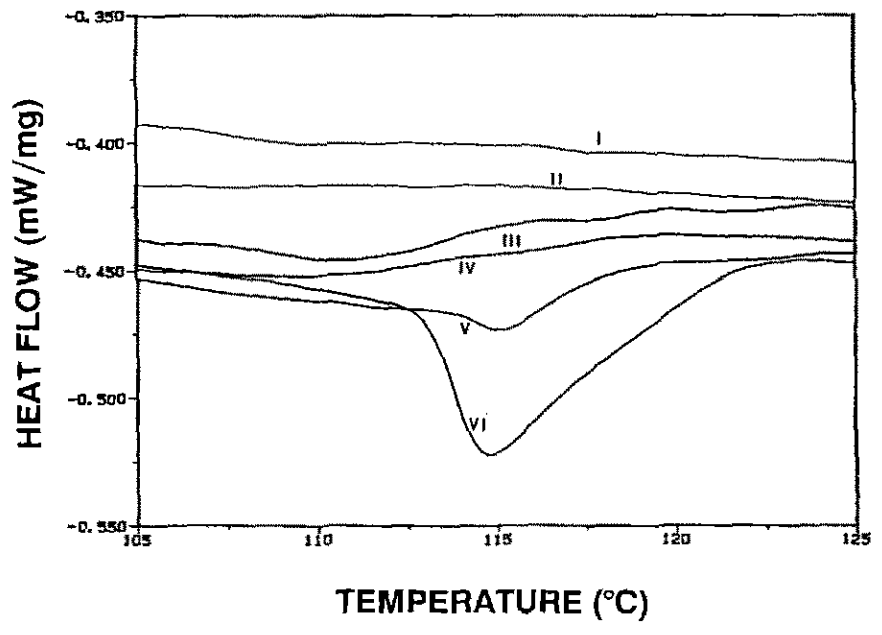

Fig. 13. DSC scans of natural rubber containing 0% SLS (curve I), 4% SLS (curve II), 8% SLS (curve III), 9% SLS (curve IV), 10% SLS (curve V) and 15% SLS (curve VI). These samples were stored at room temperature for 6 months before they were analysed.

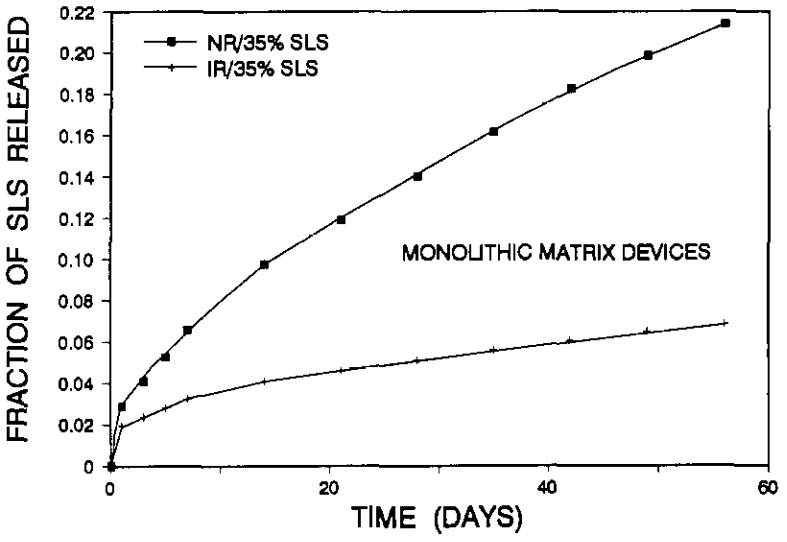

Fig. 14. The effect of the type of rubber used on the release of SLS from monolithic rubber–SLS formulations which contained 35% SLS.

different loadings of SLS was repeated after they had been stored at room temperature for 6 months. DSC thermograms of these samples showed a marked increase in the solubility limit of SLS in NR. Phase separation, i.e. the appearance of an endotherm, occurred when the level of SLS was 10%, as shown in Fig. 13. This indicated a solubility limit of 9%. These results illustrate the importance of storage time and temperature in the determination of the solubility limit of SLS in elastomers.

Studies to determine the rates of release of SLS from monolithic elastomeric matrices [16] and through elastomeric membranes [17] have shown that, at all levels of SLS, the surfactant is released more rapidly from NR formulations than from IR formulations. This is illustrated in Figs. 14 and 15 for monolithic devices and membrane devices respectively. The concept of a higher solubility limit of SLS in NR, as found in this

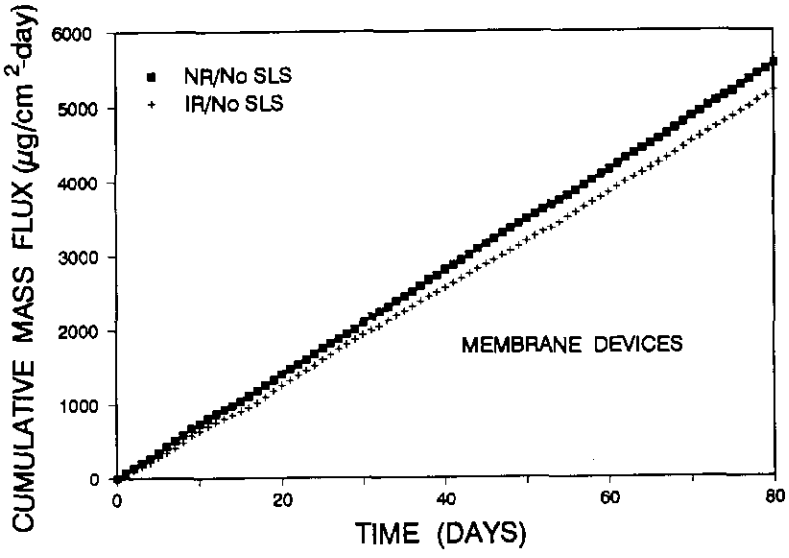

Fig. 15. Plots of cumulative mass flux against time, illustrating the effect of the type of rubber used on the mass flux of SLS through rubber membranes which initially contained no SLS.

study, presents a good explanation for the above-mentioned experimental findings.

Sodium benzoate and sorbic acid were also tested on a laboratory scale as potential inhibitors of *T. ferrooxidans*. It was found that both these compounds were more effective than SLS against *T. ferrooxidans* in cultures containing coal waste [24]. Since the solubility limit is a major factor in determining the release rate of an active agent from a controlled-release device, knowledge about the solubility limits of sodium benzoate and sorbic acid in various elastomers could assist in the design and development of controlled-release devices for long term inhibition of *T. ferrooxidans*. Future thermoanalytical studies will therefore focus on the use of DSC to determine the solubility limits of sodium benzoate and sorbic acid in elastomers.

CONCLUSIONS

(1) This study has shown that it is possible to determine the solubility limits of SLS in elastomers by DSC. Phase separation occurred when the solubility limit of SLS in a particular elastomer was exceeded. The onset of phase separation was characterized by an endotherm which appeared at 115°C.

(2) The solubility limits of SLS in the different elastomers varied. The solubility limits of SLS in natural rubber and in synthetic polyisoprene were 4% and 3% respectively, when formulations were stored at 0°C before analysis. Storage of natural-rubber formulations at room temperature for 6 months caused the solubility limit of SLS to increase to 9%. These results clearly illustrated the time and temperature dependence of the solubility of solids in elastomers.

(3) There was surprisingly little evidence, if any, in the literature on controlled-release technology of the use of DSC for determining the solubility limits of solid active agents in plastics or in elastomers. The study reported here has demonstrated the usefulness of DSC as a convenient and reliable method for determining the solubility of solids in elastomers. Future studies will focus on the determination of the solubility limits of sorbic acid and sodium benzoate in natural and synthetic rubbers by DSC.

ACKNOWLEDGEMENT

The financial support of this research by the Water Research Commission of South Africa is gratefully acknowledged.

REFERENCES

1 R.L.P. Kleinmann, The biogeochemistry of acid mine drainage and a method to control acid formation, Ph.D. Dissertation, Princeton University, Princeton, NJ, 1979.
2 P.J. Kendrick, J. Water Pollut. Control Fed., 49 (1977) 1576.
3 P.R. Dugan, Ohio J. Sci., 75 (1975) 266.
4 R.L.P. Kleinmann, D.A. Crerar and R.R. Pacelli, Min. Eng. (NY), 33 (1981) 300.
5 J.G. Thompson, Water SA, 6 (1980) 130.
6 J.M. Conradie, Growth and inhibition of *Thiobacillus ferrooxidans* in relation to acid drainage from Witwatersrand gold mine sand dumps, M.Sc. Thesis, University of Stellenbosch, Stellenbosch, South Africa, 1984.
7 M.A. Loos, J.M. Conradie, P.A. Whillier, J. Maré and C. Bosch, Research on the inhibition of bacterial oxidation of pyrite and the concomitant acid mine drainage: Part I. Investigations on gold mine sand dumps, WRC Rep. No. 132/1/90, Water Research Commission, Pretoria, South Africa, 1990.
8 P.A. Whillier, Distribution, ecology and inhibition of *Thiobacillus ferrooxidans* in relation to acid drainage from Witwatersrand gold mine dumps, M.Sc. Thesis, University of Stellenbosch, Stellenbosch, South Africa, 1987.
9 J. Maré, Distribution and inhibition of *T. ferrooxidans* in relation to acid drainage from coal waste dumps, M.Sc. Thesis, University of Stellenbosch, Stellenbosch, South Africa, 1989.
10 M.A. Loos, C. Bosch and J. Maré, Research on the inhibition of bacterial oxidation of pyrite and the concomitant acid mine drainage Part 2. Investigations on coal waste dumps, WRC Rep. No. 132/2/90, Water Research Commission, Pretoria, South Africa, 1990.
11 R.L.P. Kleinmann and P.M. Erickson, Control of acid drainage from coal refuse using anionic surfactants, U.S. Bur. Mines, Rep. Invest., RI 8847, U.S. Dept. of the Interior, Pittsburgh, PA, 1983, p. 1.
12 R.L.P. Kleinmann, Bactericidal control of acid problems in surface mines and coal refuse, Proc. Symp. on Surface Mining, Hydrology, Sedimentology, and Reclamation, Lexington, KY, 1980, p. 333.
13 P.M. Erickson, R.L.P. Kleinmann and S.J. Onysko, Control of acid mine drainage by application of bactericidal materials, U.S. Bur. Mines, Inf. Circ., IC 9027, U.S. Dept. of the Interior, Pittsburgh, PA, 1985, p. 25.
14 N.F. Cardarelli, Monolithic elastomeric materials, in A.F. Kydonieus (Ed.), Controlled Release Technologies: Methods, Theory and Applications, Vol. 1, CRC Press, Boca Raton, FL, 1980, p. 73.
15 T.J. Roseman, Monolithic polymer devices—Section 1, in A.F. Kydonieus (Ed.), Controlled Release Technologies: Methods, Theory, and Applications, Vol. 1, CRC Press, Boca Raton, FL, 1980, p. 21.
16 E. Immelman and R.D. Sanderson, Controlled release of sodium lauryl sulphate (SLS) from elastomers. I. Monolithic matrix devices, J. Controlled Release, submitted for publication.
17 E. Immelman and R.D. Sanderson, Controlled release of sodium lauryl sulphate (SLS) from elastomers. III. Membrane devices, J. Membrane Sci., submitted for publication.
18 R.W. Baker and H.K. Lonsdale, Controlled release: mechanisms and rates, in A.C. Tanquary and R.E. Lacey (Eds.), Controlled Release of Biologically Active Agents, Adv. Exp. Med. Biol., 47 (1974) 15.
19 J.H. Bishop and S.R. Silva, Antifouling paint film structure with particular reference to cross sections, Am. Chem. Soc., Div. Org. Coat. Plast. Chem., Pap., 30 (1970) 364.
20 C. Driscoll and A. Freiman, X-ray fluorescence spectrometry in antifouling coating systems, J. Paint Technol., 42 (1970) 521.

21 N.F. Cardarelli, Slow release molluscicides and related materials, in T.C. Cheng (Ed.), Molluscicides in Schistosomiasis Control, Academic Press, New York, 1974, p. 177.
22 E. Immelman and R.D. Sanderson, Research on the inhibition of bacterial oxidation of pyrite and the concomitant acid mine drainage. Part 3. Development and testing of slow release systems, WRC Rep. No. 132/3/90, Water Research Commission, Pretoria, South Africa, 1990, p. 82.
23 Aldrich Chemical Catalog, Aldrich Chemical Company, Milwaukee, WI, 1986/87, p. 594.
24 M.A. Loos, C. Bosch, J. Maré, E. Immelman and R.D. Sanderson, Evaluation of sodium lauryl sulphate, sodium benzoate and sorbic acid as inhibitors of acidification of South African coal waste, Proc. 5th Ground Water Symposium: Ground Water and Mining, Randburg, South Africa, 31 July–5 August 1989, Geol. Soc. South Africa, 1989, p. 193.